RESEARCH PAPER

Development of PMMA/TiO_2 Nanocomposites and Study Morphology, Optical, Thermal (DSC) and Biological Properties

Suhad Aloon Abdullh *, **Rana S. Mahmood**

Ministry of Education, Diyala Education Directorate, Diyala, Baqubah, 32001, Iraq

ARTICLE INFO

Article History:
Received 14 May 2026
Accepted 06 July 2026
Published 01 October 2026

Keywords:
Casting method
DSC
FESEM
PMMA
TiO_2 nanoparticles

ABSTRACT

This work examines the production of PMMA/TiO_2 nanocomposites and investigates their morphological, optical, thermal, and biological properties. The nanocomposites were synthesized by incorporating 5 wt% of TiO_2 nanoparticles into a PMMA matrix via a casting technique. Morphological examination demonstrated the distribution and interaction of TiO_2 nanoparticles inside the polymer matrix, signifying enhanced structural homogeneity at these concentrations. The optical properties were examined by UV-Vis spectroscopy, revealing notable alterations in absorption characteristics and a reduction in the optical band gap with the incorporation of TiO_2 nanoparticles. The thermal behavior was assessed via differential scanning calorimetry (DSC), revealing enhanced thermal stability and a modification in the glass transition temperature (Tg) to (104.7 °C) attributable to the nanoparticles' presence. Moreover, biological assays demonstrated that the nanocomposites possess superior antibacterial efficacy relative to pure PMMA, owing to the inherent characteristics of the TiO_2 nanoparticles. The findings indicate that the PMMA/TiO_2 nanocomposites exhibit improved multifunctional characteristics. This renders it a promising contender for applications in biology, optics, and innovative materials.

How to cite this article
Abdullh S., Mahmood R. Development of PMMA/TiO_2 Nanocomposites and Study Morphology, Optical, Thermal (DSC) and Biological Properties. J Nanostruct, 2026; 16(4):4698-4709. DOI: 10.22052/JNS.2026.04.019

INTRODUCTION

Although numerous studies have addressed PMMA/TiO_2 nanocomposites and their diverse properties, many have focused on a specific aspect without comprehensively integrating structural, optical, thermal, and biological properties. [1,2] Furthermore, the effect of adding TiO_2 nanoparticles at different concentrations on improving PMMA polymer performance still requires further investigation and the exploration of alternative preparation methods. [3] Therefore, the novelty of this study lies in its preparation of PMMA/TiO_2 nanocomposites and the investigation of the effect of TiO_2 nanoparticles on morphological, optical, and thermal properties using DSC technology, in addition to evaluating biological properties using the casting method. The aim is to develop multifunctional nanomaterials that can be used in advanced medical and optical applications. Polymers such as plastics and rubbers pervade our lives, and we come across them in many dierent forms. Their physical properties are therefore of great importance, and an understanding of them is vital for their use

* Corresponding Author Email: ranasaadmahmood82@gmail.com

in technology and engineering [4]. Composite materials constitute an advanced engineering system wherein two or more components of differing characteristics are combined to achieve performance attributes that surpass those of the individual pieces [5]. Historically, reinforcement has been supplied by constituents such as fibers, whiskers, or particulates in metals, ceramics, or polymers, improving mechanical, thermal, and chemical properties for diverse applications, including aerospace, structural materials, biomedical devices, and energy technologies [6,7]. Polymethyl methacrylate (PMMA) is produced via the free radical polymerization of methyl methacrylate and is distinguished by its colorless and transparent characteristics. The light transmittance surpasses that of other polymers. Additionally, it is lightweight, durable, demonstrates significant mechanical strength at room temperature, has low water absorption, is resistant to water and specific dilute acids and inorganic salts, endures long-chain alkanes and ethers, is non-toxic, and is flame-retardant upon ignition [8]. The fabrication of composite materials using nanoparticles poses difficulties in attaining a homogeneous particle distribution inside the matrix; nonetheless, it facilitates the creation of composites with varied properties for practical uses. These composites consist of one or more types of nanoparticles of diverse shapes and sizes integrated inside the matrix material. They differ from traditional composites in the distribution of the integrated components, which is partially random yet controlled. The nanocomposites demonstrate isotropy, indicating that their properties are consistent in all directions. This reinforcement approach enables particles to distribute the load with the matrix material, so augmenting its stiffness, creep resistance, impact strength, and resistance to wear and fatigue, while also conferring specialized attributes to achieve the intended goals [9,10]. Metal oxides (including TiO2 [11,12], SiO2, and ZnO [13]) and carbon-based nanofillers have been extensively studied to improve structural, electrical, and optical characteristics [14,15]. The effectiveness of these reinforcements is highly dependent on establishing uniform dispersion throughout the matrix and managing interfacial interactions that control stress transfer and property development [16]. TiO2 nanoparticles have attracted considerable attention owing to their several advantages, such as a high refractive index, photoactivity throughout the UV spectrum, and UV absorption properties, for instance [17]. Their integration into PMMA matrices has been shown to enhance thermal stability, elevate Tg, and augment optical properties as well [18]. The surface characteristics of these oxide nanoparticle species are hydrophilic owing to the presence of hydroxyl groups [19]. To effectively disseminate the nanoparticle within a hydrophobic polymer matrix, enhancement of the interfacial interaction is essential. Modification of the nanoparticle surface via various interfacial techniques has been implemented. These procedures entail the encapsulation of nanoparticles through emulsion polymerization in PMMA [20]. Nonetheless, TiO_2 nanoparticles have significant polarity and elevated surface energy; thus, they may agglomerate at increased loading levels, diminishing their reinforcing efficacy. This challenge has prompted endeavors to alter surface particles to reduce particle-particle interactions and enhance uniform distribution inside the organic matrix. Utilizing these approaches, PMMA/TiO_2 nanocomposites exhibit enhanced performance in structural and functional applications across optical, electrical, and biological domains [21]. The Minimum Inhibitory Concentration (MIC) is the lowest concentration of an antimicrobial drug that inhibits observable growth of a microbe following a certain incubation period. The microtiter plate (MTP) broth microdilution method is a prevalent technique for determining minimum inhibitory concentration (MIC) due to its rapidity, cost-effectiveness, reproducibility, and high-throughput capability, enabling the simultaneous testing of numerous isolates and concentrations in a 96-well plate. In MTP MIC testing, bacterial growth is assessed in liquid medium across a serial dilution series of the tested compound(s). Growth can be read by turbidity/optical density, but many laboratories use colorimetric viability indicators to improve clarity—especially when extracts, nanoparticles, or colored compounds may interfere with turbidity assessment. Resazurin is a redox dye used as a cell viability indicator. In its oxidized form, it appears blue/purple; metabolically active (viable) bacteria reduce it to resorufin, which becomes pink (and may further reduce to a colorless form in strongly reducing conditions). Therefore: Blue/purple = no detectable metabolic activity (growth inhibited) and Pink = active metabolism (growth present).

Using resazurin provides a clear endpoint for MIC determination, especially when broth becomes slightly cloudy or when test agents affect optical readings [22,23]. In this research, PMMA/TiO2 nanofilms will be fabricated and the effect of titanium on their structural, morphological and biological properties will be studied.

MATERIALS AND METHODS

Materials Used

Poly(methyl methacrylate) (PMMA) [$CH_2C(CH_3)(CO_2CH_3)$] – ~800,000 g/mol – A vonchem Ltd., UK, Chloroform [$CHCl_3$]– 119.38 g/mol – ACS Chemicals, India – 99%.

Preparation of PMMA/TiO_2 Nanofilms

The solution-casting method was used to make the composite nanofilms. To make a very uniform solution, 1 g of PMMA granules was completely dissolved in 40 mL of chloroform in a glass beaker with magnetic stirring at 25 °C for 1 hour. We took 10 mL of this solution and used it as a base polymer to make more composite structures. The amount of TiO_2 nanoparticles added to the PMMA solution ranged from 5 wt%. Ultrasonic treatment was applied to the suspensions for 8 minutes to ensure equal distribution of nanoparticles and inhibit agglomeration. When you get the nanoparticle suspension.

Characterization Tests

Utilizing a ZEISS SIGMA VP field emission scanning electron microscope (FESEM) type. Absorption spectra and Surface Plasmon Resonance (SPR) were obtained for colloids using a Double Beam 1800 UV Spectrometer produced by Shimadzu, Japan, together with Differential Scanning Calorimetry (DSC) analysis. The thermal properties of the fabricated films were analyzed using differential scanning calorimetry (STA. PT-1000 Linseis). The system was calibrated with 9-19 mg of alumina at a temperature ramp rate of 10°C/min in the presence of argon gas.

Antioxidant Activity by DPPH Free Radical Scavenging Assay

The DPPH radical scavenging experiment was used to test how well the nano-compounds worked as antioxidants, as described in [24]. We made a new 0.1 mM DPPH solution in methanol. One milliliter of each nano-compound was added to one milliliter of DPPH solution at concentrations above, at, and below the MIC. The mixtures were kept in the dark at room temperature for 30 minutes, and the absorbance was measured at 517 nm. Ascorbic acid was the positive control. We used the formula [24] to figure out the percentage of radical scavenging activity.

$$\% \text{ Scavenging activity} = 100 \times [(A_{control} - A_{sample}) / A_{control}]$$

Where, $A_{control}$ is the absorbance of DPPH solution without sample, A_{sample} is the absorbance

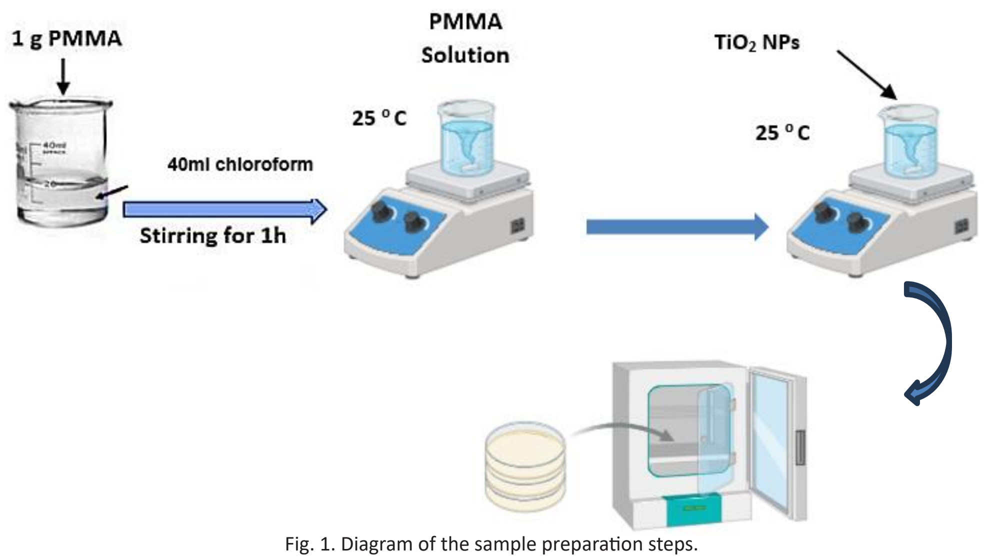

Fig. 1. Diagram of the sample preparation steps.

with the test compound.

Materials

Consumables: Sterile 96-well flat-bottom microtiter plates with lid, Sterile microtubes (1.5–2 mL) and Sterile pipette tips (10, 200, 1000 µL). Reagents & Media: Mueller–Hinton Broth (MHB), Solvent for stock preparation (e.g., sterile water / DMSO) and Resazurin solution (commonly prepared as 0.01–0.02% w/v; see below). Microbiology items: Fresh bacterial culture (18–24 h) on suitable agar. Equipment: Micropipettes (10–100 µL, 100–1000 µL) and Incubator at 35–37°C.

Methods (Broth Microdilution MIC by MTP using Resazurin)

A) Preparation of stock solutions: Prepare a concentrated stock of each tested agent.

B) Preparation of resazurin working solution

A commonly used approach:

Prepare 0.01% w/v resazurin in sterile distilled water (e.g., 10 mg in 100 mL).

Mix until dissolved, filter sterilize, and store protected from light (amber tube) at 4°C.

C) Standardization of bacterial inoculum

Pick 3–5 well-isolated colonies from a fresh agar plate (18–24 h).

Suspend in saline/MHB to match 0.5 McFarland (≈1–2 × 10^8 CFU/mL for many bacteria).

Dilute this suspension in MHB to obtain the final inoculum used in wells.

Typical final inoculum in each well is around 5 × 10^5 CFU/mL.

Keep inoculum fresh and use within a short time (avoid long standing).

D) Plate setup (example workflow)

Dispense broth: Add 100 µL MHB to all test wells that will contain dilutions.

Prepare serial two-fold dilutions (2× dilutions)

There are two common ways:

Method 1 (in-plate serial dilution):

Add 100 µL of the test agent at the highest concentration to the first well of the dilution row/column.

Mix well (pipette up/down 5–8 times).

Transfer 100 µL from the first well to the next well (already containing 100 µL broth) to make a two-fold dilution.

Continue across the row/column.

Discard 100 µL from the last well to equalize volumes.

Method 2 (pre-dilution in tubes then dispense):

Prepare the two-fold dilution series in tubes, then add equal volumes to plate wells.

3) Add bacterial inoculum

Add 100 µL of the prepared inoculum to each well containing 100 µL of the diluted agent.

Final volume per well becomes 200 µL.

This ensures the test agent concentration is at the intended final level (because dilutions were made assuming this final volume).

E) Controls (essential)

Include these controls in every plate:

Sterility control (Media only):

MHB (no bacteria, no agent).

Confirms no contamination.

Growth control (Positive control):

MHB + bacteria (no agent).

Confirms organism viability and adequate growth.

F) Incubation

Cover the plate and incubate at 35–37°C for 18–24 hours (typical for many bacteria).

Avoid shaking (shaking may change nanoparticle behavior).

G) Resazurin addition and second incubation

After the main incubation, add 10–20 µL of resazurin working solution to each well (keep it consistent).

Incubate again at 35–37°C for 1–3 hours (time depends on organism metabolic rate and inoculum).

Protect the plate from strong light if possible.

H) Reading results and determining MIC

Visual endpoint:

Pink wells = growth (viable bacteria).

Blue/purple wells = no detectable growth/metabolic activity.

MIC definition:

The MIC is the lowest concentration of the tested agent at which the well remains blue/purple (i.e., no color change to pink) compared with the growth control.

RESULTS AND DISCUSSION

Field-emission scanning electron microscopy (FESEM) images of PMMA and composites Morphological analysis was performed using FESEM images shown in Figs. 2 and 3. Particle strengthening effects in composites play a crucial role in determining their physical properties [2]. The field emission scanning electron microscopy (FESEM) images in Fig. 2 of the PMMA film show a smooth, spherical surface, consistent with a uniform distribution across the surface. Fig. 3 show the PMMA/TiO_2 composition with weight percentages (5 wt%) of TiO_2 loaded into the PMMA matrix. It is noted that the 5 wt% PMMA/TiO_2 mixture film indicates that the TiO_2 nanoparticles are uniformly distributed across the PMMA matrix. They appear as small granules, We observe that the 5% PMMA/TiO_2 film has a lumpy structure

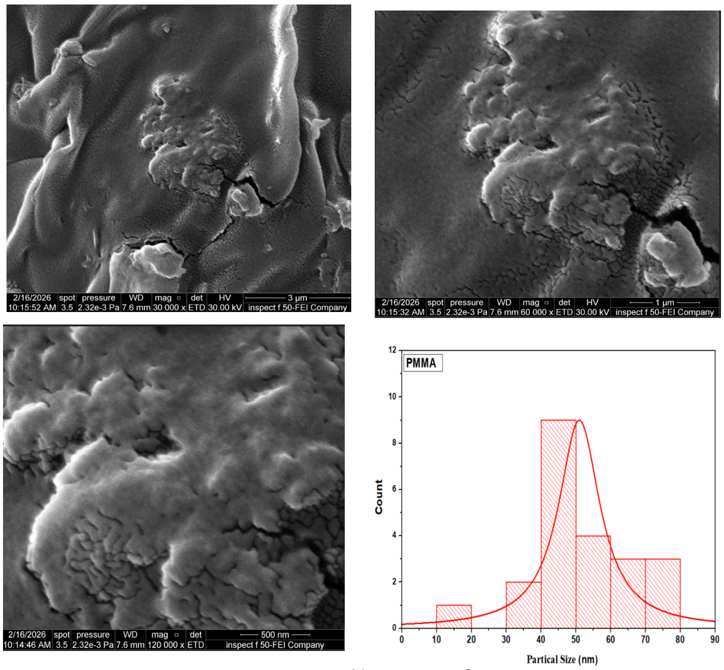

Fig. 2. FESEM images and histogram of PMMA Pure.

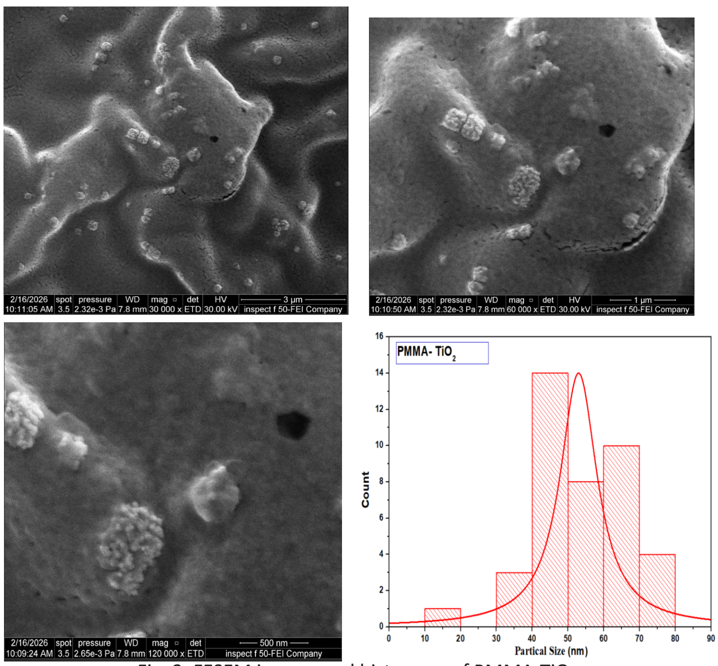

Fig. 3. FESEM images and histogram of PMMA-TiO_2.

with small granules on the surface. Adding TiO_2 to the PMMA polymer matrix indicates changes in the morphology, which may improve its physical properties [26-28].

Optical Properties Results

Ultraviolet and visible spectroscopy is used to study the optical properties of (PMMA)/TiO2 composite nanofilms with varying content of TiO2 nanoparticles. Fig. 4 shows the surface plasmon resonance peaks (SPR) obtained for the colloidal solutions of TiO_2 nanoparticles as they were nearly constant from (289nm). The UV–Visible absorption spectrum of the PMMA/TiO2 nanocomposite thin films is shown in Fig.4.

The energy gap (Eg) for the allowed indirect transition was calculated using equation [29]:

$$\alpha h\upsilon \approx B(h\upsilon - Eg)^{1/2} \quad (1)$$

A tangent is drawn from the best straight line that crosses most points beyond the absorption edge. Table 3 shows the energy gap values for all of the composite films. The table shows that the energy gap value for the pure PMMA film is (4.67) eV. However, when 5wt% TiO_2 are added, the energy gap value goes down a little. This result is in line with what was found in earlier studies. Adding small amounts of reinforcement material to the base material (PMMA) makes the energy gap value lower. This is because the reinforcement material makes groups of transmitted charge. These clusters improve electrical conductivity by adding more charges. Moreover, the presence of different reinforcement materials leads the reinforced molecules to close the gap between two local energy levels. This lowers the potential barrier and makes it easier for charge carriers to move between these levels [30].

Differential Scanning Calorimetry (DSC)

One of the properties of glass in polymers is that their mechanical and physical properties change at a certain temperature called the resistance to glass transition, which is usually denoted by (Tg). It can be defined as the temperature at which a polymer changes from a strong, rigid material to a flexible material above the glass transition,

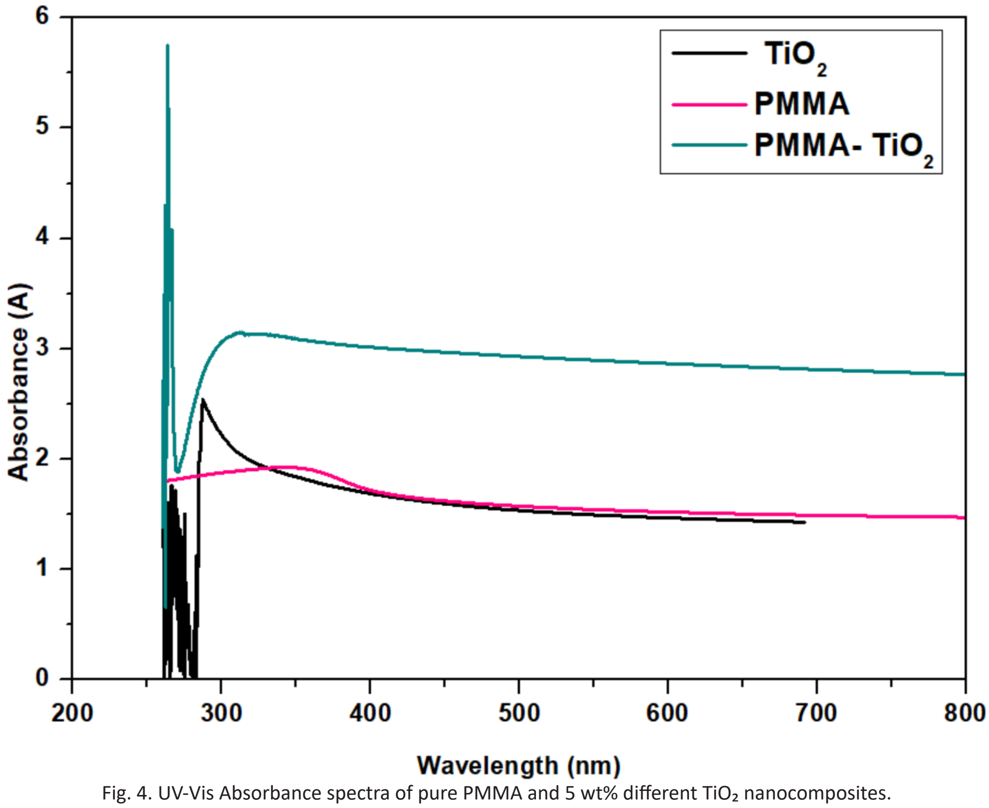

Fig. 4. UV-Vis Absorbance spectra of pure PMMA and 5 wt% different TiO_2 nanocomposites.

becoming a flexible polymer. [31]

Plastics possess a range of different transformations (transitions) under the influence of high temperature. When purified at a soft temperature below the glass transition point, the plastic material is a rigid solid. Upon transition, it transforms into an elastic plastic material, and then into an elastic state in the case of a non-ductile plastic, and into a highly viscous liquid in the case of a thermoplastic plastic [32]. The glass transition point depends on the number of atoms and molecules in the plastic material. Therefore, the more complex the structure, the greater the capacitance, and the higher the maximum weight possessed by the plastic material, the higher its transition point.

The glass transition temperature of the pure PMMA polymer films reinforced with 5wt % titanium oxide nanoparticles was calculated using a differential calorimeter (DSC). Fig. 6 shows the glass transition temperature values of the prepared films, where we note that the glass transition temperature value of the pure PMMA film is (104.7 ºC) [32]. Studies indicate that adding

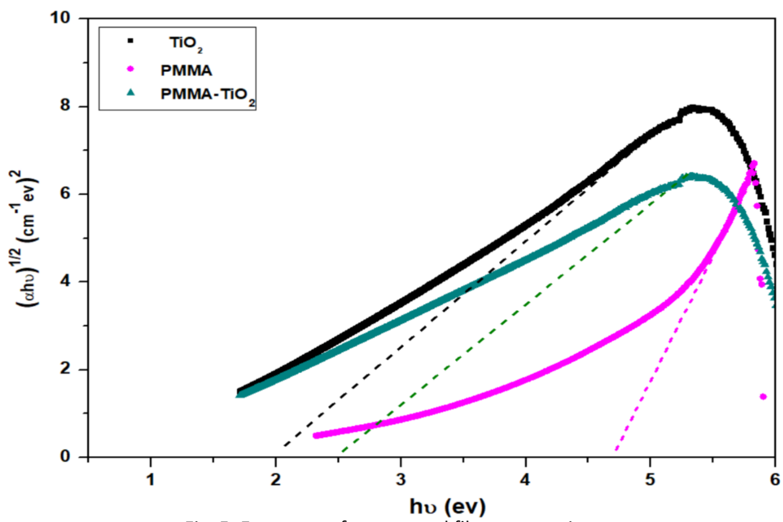

Fig. 5. Energy gap for prepared films composites.

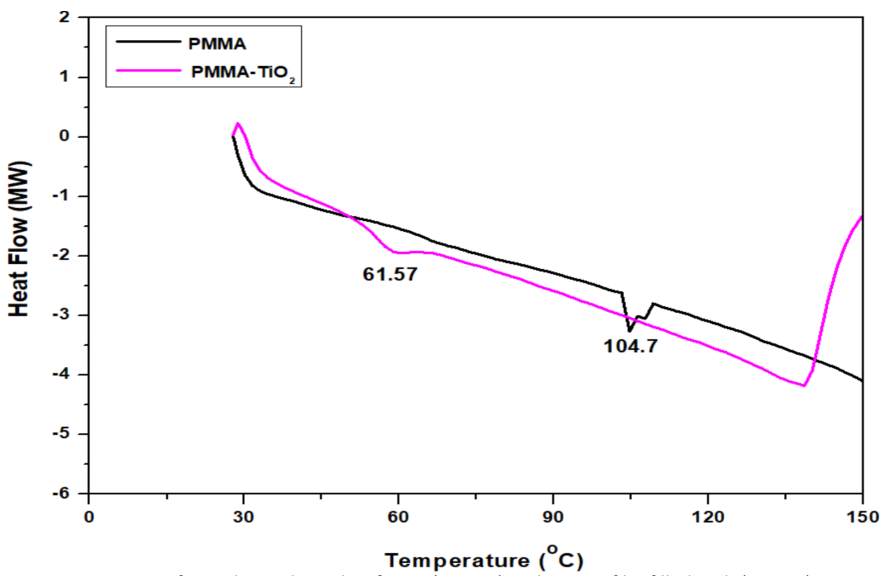

Fig. 6. Diagram of DSC thermal weight of pure (PMMA) and PMMA film filled with (5 wt.%) TiO_2.

TiO_2 nanoparticles to polymethyl methacrylate (PMMA) alters the glass transition temperature (Tg), with the value depending on the filler ratio and the preparation method. It has been observed that Tg can fall within a range of 60–70 °C in some modified systems, showing a slight increase or decrease compared to the pure polymer, due to the interaction between the polymer chains and the nanoparticles.[33] Several recent studies have shown that the introduction of TiO_2 improves thermal stability and affects the mobility of polymer chains, leading to a wide range of Tg values that can be either low or high compared to the pure polymer [34].

Application biology

Table 2 presents the statistical analysis of the DPPH radical scavenging activity of TiO_2 nanoparticles at three tested concentrations. The findings reveal a clear concentration-dependent antioxidant effect, with a highly significant overall difference among concentrations ($P < 0.001$). The highest concentration (1000 µg/ml) showed the greatest scavenging activity, with a mean

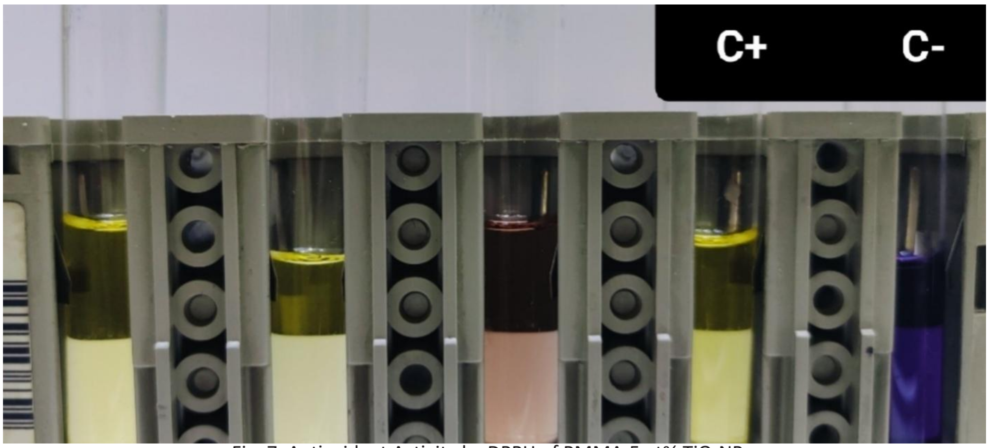

Fig. 7. Antioxidant Activity by DPPH of PMMA-5wt% TiO_2NPs.

Table 1. Data replicate absorbance and DPPH inhibition values of PMMA- 5wt% TiO_2 NPs.

Concentration	Replicate	Absorbance	Inhibition %
1000 µg/ml	1	0.267	84.00
1000 µg/ml	2	0.284	82.98
1000 µg/ml	3	0.251	84.96
500 µg/ml	1	0.317	81.01
500 µg/ml	2	0.334	79.99
500 µg/ml	3	0.301	81.97
250 µg/ml	1	0.901	46.01
250 µg/ml	2	0.922	44.76
250 µg/ml	3	0.884	47.03

Table 2. statistical analysis of DPPH radical scavenging activity of PMMA- 5wt% TiO2 NPs at different concentrations.

Concentration	Parameter	Mean ± SD	P-value	Significance
1000 µg/ml	Inhibition %	83.98 ± 0.99^a	<0.001	Significant
500 µg/ml	Inhibition %	80.99 ± 0.99^b		
250 µg/ml	Inhibition %	45.93 ± 1.14^c		

inhibition percentage of 83.98 ± 0.99%, followed by 500 µg/ml (80.99 ± 0.99%), whereas the lowest concentration (250 µg/ml) exhibited a markedly lower activity (45.93 ± 1.14%). The distinct superscript letters indicate that each concentration differed significantly from the others, confirming that the antioxidant capacity declined significantly as the concentration decreased. This trend is consistent with the principle of the DPPH assay, in which higher scavenging percentages reflect a greater ability of the tested material to donate electrons or hydrogen atoms to neutralize free radicals [35,36].

From a functional perspective, the high inhibition values observed at 1000 and 500 µg/ml suggest that the tested TiO_2 nanoparticles possessed substantial in vitro antioxidant potential within the upper concentration range. The relatively small difference between these two concentrations indicates that the nanoparticles retained a high level of radical scavenging efficiency even after a twofold reduction in concentration. In contrast, the marked decline at 250 µg/ml suggests that the antioxidant response became considerably weaker once the nanoparticle concentration dropped below a more effective threshold. Similar concentration-dependent patterns have been described for TiO_2 nanoparticles in previous studies, particularly in green-synthesized systems, where antioxidant activity increased with dose and was influenced by nanoparticle size, surface chemistry, and synthesis-associated bioactive residues [37,38]

The strong activity recorded at 1000 µg/ml is particularly noteworthy because it approaches the level usually associated with potent antioxidant systems in DPPH assays. Although TiO_2 is more commonly discussed in relation to photocatalytic and surface-reactive properties, an increasing body of evidence indicates that TiO_2 nanoparticles can also exhibit appreciable antioxidant behavior under in vitro chemical assay conditions, especially when synthesized through biological or plant-mediated routes. In such systems, the observed scavenging effect may reflect not only the physicochemical characteristics of the TiO_2 core itself but also the contribution of surface-bound organic compounds that enhance redox reactivity [37].

The MIC-based susceptibility ranking demonstrated that the tested microorganisms differed clearly in their response to TiO_2 nanoparticles, indicating variable antimicrobial sensitivity across bacterial and fungal species. Among all tested organisms, *Streptococcus pyogenes* and *Candida albicans* showed the highest susceptibility, each with an MIC of 16 µg/ml, whereas *Escherichia coli* showed an intermediate response with an MIC of 32 µg/ml. In contrast, *Staphylococcus aureus* and *Klebsiella pneumoniae* exhibited the lowest susceptibility, both requiring 64 µg/ml for growth inhibition. Since lower MIC values reflect greater antimicrobial potency, these results indicate that TiO_2 nanoparticles were most effective against *S. pyogenes* and *C. albicans*, moderately effective against *E. coli*, and comparatively less effective against *S. aureus* and *K. pneumoniae*. This general interpretation is consistent with the established use of MIC values as a quantitative indicator of antimicrobial activity, where lower concentrations indicate stronger inhibitory performance [39,40].

The strong susceptibility of *S. pyogenes* to TiO_2 nanoparticles is biologically plausible, as Gram-positive organisms can be highly affected by nanoparticle-mediated membrane disruption, oxidative stress, and surface interaction, although susceptibility patterns are not always uniform across all Gram-positive bacteria. The lower MIC observed for *S. pyogenes* compared with *S. aureus* in the present results suggests that species-specific surface properties, metabolic behavior, or differences in the interaction between nanoparticles and cell envelope structures may have influenced the antimicrobial response. Reviews of TiO_2 nanoparticle antimicrobial activity have similarly noted that susceptibility cannot be predicted solely on the basis of Gram reaction, because microbial sensitivity depends on multiple factors, including nanoparticle size, surface charge, crystallinity, and the physiological properties of the target organism [40,41].

The antifungal result against *Candida albicans* is also noteworthy. The MIC of 16 µg/ml places *C. albicans* among the most susceptible tested organisms, suggesting that TiO_2 nanoparticles possessed appreciable antifungal activity in addition to their antibacterial effects. This broad-spectrum performance agrees with previous reports showing that TiO_2-based nanomaterials can inhibit fungal cells through oxidative stress generation, membrane-associated damage, and interference with essential cellular processes. Published evidence has likewise highlighted that TiO_2 nanoparticles may act against *Candida* species and other fungi, especially when the particles possess high surface reactivity or are used in formulations optimized for antimicrobial performance [42,43].

The intermediate susceptibility of *E. coli*, with an MIC of 32 µg/ml, suggests that TiO_2 nanoparticles were also active against this Gram-negative bacterium, although to a lesser extent than against *S. pyogenes* and *C. albicans*. This observation is important because Gram-negative bacteria are often considered more difficult to inhibit due to the presence of an outer membrane that can limit the penetration of antimicrobial agents. Nevertheless, TiO_2 nanoparticles may still exert inhibitory effects against such bacteria through direct contact, reactive oxygen species generation, and destabilization of membrane integrity. Previous studies have reported antimicrobial activity of TiO_2 nanoparticles against

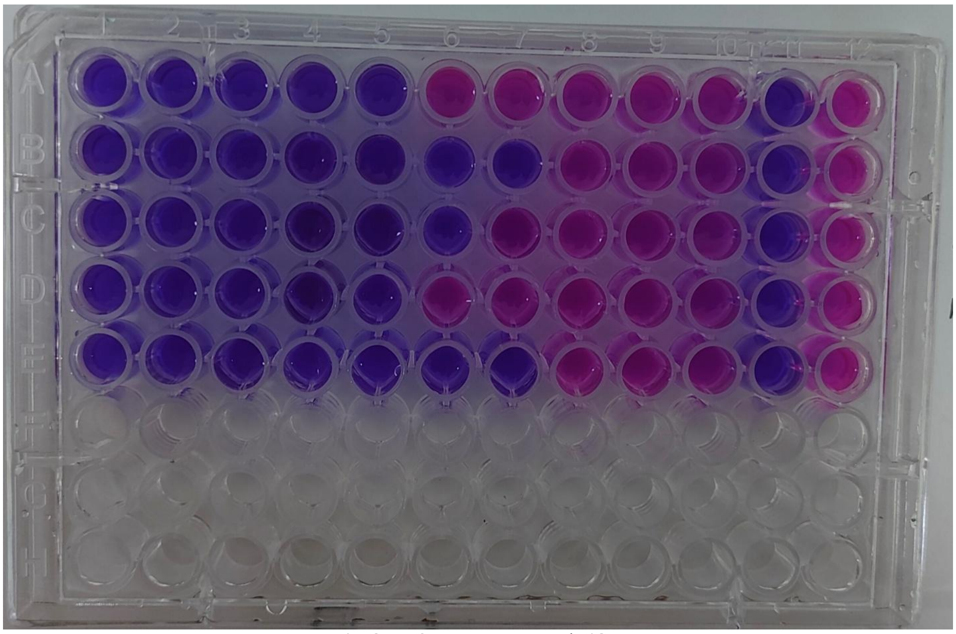

Fig. 8. MIC to PMMA- 5wt% TiO_2.

Table 3. Comparative MIC and fold-difference ranking of the tested isolates to PMMA- 5wt% TiO_2.

Rank	Isolate	Microbial group	MIC (µg/ml)	Fold difference vs lowest MIC	Interpretation
1	*S. pyogenes*	Gram-positive bacteria	16	1	Highest susceptibility
1	*C. albicans*	Fungi	16	1	Highest susceptibility
2	*E. coli*	Gram-negative bacteria	32	2	Intermediate susceptibility
3	*S. aureus*	Gram-positive bacteria	64	4	Lower susceptibility
3	*K. pneumoniae*	Gram-negative bacteria	64	4	Lower susceptibility

Table 4. value of MIC to PMMA- 5wt% TiO_2.

PMMA-5wt% TiO2		MIC (µg/ml)
Gram positive bacteria	*S. aureus*	64
	S. pyogenes	16
Gram negative bacteria	*E. coli*	32
	K. pneumoniae	64
Fungi	*C. albicans*	16

E. coli, supporting the interpretation that the present result reflects genuine inhibitory potential rather than an isolated finding [44,40].

By contrast, *S. aureus* and *K. pneumoniae* showed the highest MIC values (64 µg/ml), indicating the lowest susceptibility among the tested isolates. Although these MICs still reflect measurable antimicrobial activity, they suggest that higher nanoparticle concentrations were necessary to achieve inhibition in these organisms. In the case of *K. pneumoniae*, this may be related to the known structural and protective features of Gram-negative pathogens, including the outer membrane and, in some strains, capsule-associated defense. For *S. aureus*, the reduced sensitivity relative to *S. pyogenes* may reflect species-level differences in tolerance to oxidative or membrane-active stress. Similar variability among bacterial species has been reported in previous TiO_2 nanoparticle studies, emphasizing that antimicrobial performance may differ considerably depending on the target organism and the physicochemical characteristics of the nanoparticles used [45,40].

Overall, this table demonstrates that the antimicrobial activity of TiO_2 nanoparticles was species-dependent, with the strongest effect observed against *S. pyogenes* and *C. albicans*, moderate activity against *E. coli*, and lower activity against *S. aureus* and *K. pneumoniae*. The fold-difference values further emphasize this pattern, showing that the least susceptible organisms required four times the MIC needed for the most susceptible ones. Collectively, these findings support the conclusion that TiO_2 nanoparticles possess broad antimicrobial potential, but that their inhibitory efficiency varies according to the biological characteristics of the target microorganism and the interaction between the nanoparticle surface and microbial cell structures [40,46].

CONCLUSION

This study's results indicated that the integration of titanium dioxide nanoparticles (at 5 wt%) into a polymethyl methacrylate (PMMA) matrix effectively yielded multifunctional nanocomposites with improved optical and functional characteristics. Field emission scanning electron microscopy (FESEM) coupled with ImageJ analysis shown that augmenting the TiO_2 loading, especially at 0.6 g, promoted uniform dispersion and diminished agglomeration, resulting in a reduction of particle sizes from approximately 52.88 nm to around 40 nm. The composites demonstrated superior thermal stability compared to pure PMMA, while there was no alteration in the glass transition temperature (Tg) between the polymer and the composites. This study established that free radicals can be employed in the 2,2-diphenyl-1-picrylhydrazyl (DPPH) assay to assess the capacity of materials to function as free radical scavengers or hydrogen donors, offering a speedy, straightforward, and cost-effective approach for evaluating antioxidant capabilities. The DPPH analysis approach employs a low concentration of DPPH, a stable free radical. The DPPH free radical interacts with a single electron, resulting in absorption at a peak wavelength of 517 nm (violet hue). Antioxidants interact with DPPH, in the presence of a hydrogen donor (e.g., a free radical scavenger), converting DPPH to DPPHH and diminishing DPPH absorption. In contrast to the DPPH-H form, decolorization (i.e., yellowing) transpires with an increase in electron acquisition. The decolorization capability correlates with the diminishing capacity. The synthesized PMMA/titanium dioxide nanoparticles exhibit antibacterial characteristics.

CONFLICT OF INTEREST

The authors declare that there is no conflict of interests regarding the publication of this manuscript.

REFERENCES

1. Alharbi ND, Moselhy MTH, Guirguis OW. Impact of doping different concentrations of TiO_2 nanoparticles to PMMA on its structural, thermal and optical properties for optical applications. Journal of Non-Crystalline Solids. 2025;661:123558.
2. Saeed A, Alzahrani E, Morsi MA, Tarabiah AE, Abdelrazek EM, Aldwais S, et al. Enhanced optical and electrical properties of PEO/PMMA/TiO_2 nanocomposites for optoelectronic applications. Opt Mater. 2024;157:116402.
3. Lyly Nyl I, Aziz AF, Habibah Z, Zaihidi MM, Abdullah MH, Herman SH, et al. Optical Properties and Surface Morphology of PMMA:TiO_2 Nanocomposite Thin Films. Advanced Materials Research. 2011;364:105-109.
4. Mahmood RS, Salman SA, Bakr NA. The electrical and mechanical properties of Cadmium chloride reinforced PVA:PVP blend films. Papers in Physics. 2020;12:120006.
5. Simões S. High-Performance Advanced Composites in Multifunctional Material Design: State of the Art, Challenges, and Future Directions. Materials. 2024;17(23):5997.
6. Kumar A, Dixit S, Singh S, Sreenivasa S, Bains PS, Sharma R. Recent developments in the mechanical properties and recycling of fiber-reinforced polymer composites. Polym Compos. 2024;46(5):3883-3908.
7. Mohammed HO. Preparation, Optimization, and Characterization of PMMA/TiO_2–Saffron Dye Nanocomposites: Structural and Physical

Properties. JOURNAL OF UNIVERSITY OF BABYLON for Pure and Applied Sciences. 2026;33(4):157-173.

8. Salloomi N, Hussien Ali N, S. Rasheed H, J. Alwan T. Nanofibers of PMMA/TiO_2 Produced by Electrospinning. Mustansiriyah Journal of Pure and Applied Sciences. 2025;3(1):117-122.
9. Khdary NH, Almuarqab BT, El Enany G. Nanoparticle-Embedded Polymers and Their Applications: A Review. Membranes. 2023;13(5):537.
10. Saleh HM, Hassan AI. Synthesis and Characterization of Nanomaterials for Application in Cost-Effective Electrochemical Devices. Sustainability. 2023;15(14):10891.
11. Aubad MJ, Khafaji SOW, Hussein MT, Al-Shujairi MA. Modal analysis and transient response of axially functionally graded (AFG) beam using finite element method. Materials Research Express. 2019;6(10):1065g1064.
12. Sattar S, Alaiwi Y, Radhi NS, Al-Khafaji Z, Al-Hashimi O, Alzahrani H, et al. Corrosion reduction in steam turbine blades using nano-composite coating. Journal of King Saud University - Science. 2023;35(8):102861.
13. Sallal HA, Mahboba MH, Radhi MS, Hanif A, Al-Khafaji ZS, Ahmad S, et al. Effect of adding (ZrO_2-ZnO) nanopowder on the polymer blend (lamination and methyl vinyl silicone) in a hybrid nanocomposite material. Journal of King Saud University - Science. 2024;36(2):103061.
14. Abeer Adnan A, Zainab A-K. Study the Effect of Adding Malic Anhydride and Carbon Fibers to the Mechanical and Morphology Properties of Polypropylene. Journal of Advanced Research in Micro and Nano Engineering. 2024;23(1):16-25.
15. Radhi NS, Salman AJ, Al-Khafaji Z. Investigation of in vitro behavior of composite coating hydroxyapatite-nano silver on 316L stainless steel substrate by electrophoretic technic for biomedical tools. Open Engineering. 2024;14(1).
16. Zhong Z, Jiang X, Sun H, Wu Z, Yang L, Matamoros-Veloza A. Recent Research on the Optimization of Interfacial Structure and Interfacial Interaction Mechanisms of Metal Matrix Composites: A Review. Adv Eng Mater. 2024;26(23).
17. Lettieri S, Pavone M, Fioravanti A, Santamaria Amato L, Maddalena P. Charge Carrier Processes and Optical Properties in TiO_2 and TiO_2-Based Heterojunction Photocatalysts: A Review. Materials. 2021;14(7):1645.
18. Lin C-K, Xie J-W, Tsai P-J, Wang H-Y, Lu Z-W, Lin T-Y, et al. The Effects of Different Blending Methods on the Thermal, Mechanical, and Optical Properties of PMMA/SiO_2 Composites. Journal of Composites Science. 2024;8(9):369.
19. Diebold U. The surface science of titanium dioxide. Surf Sci Rep. 2003;48(5-8):53-229.
20. Lin K-F, Lin K-J. PMMA-based Montmorillonite Nanocomposites by Soap-free Emulsion Polymerization. Polymer Nanocomposites by Emulsion and Suspension Polymerization: The Royal Society of Chemistry; 2010. p. 78-110. http://dx.doi.org/10.1039/9781849732192-00078
21. Khan I, Saeed K, Khan I. Nanoparticles: Properties, applications and toxicities. Arabian Journal of Chemistry. 2019;12(7):908-931.
22. Balouiri M, Sadiki M, Ibnsouda SK. Methods for in vitro evaluating antimicrobial activity: A review. Journal of Pharmaceutical Analysis. 2016;6(2):71-79.
23. Serov DA, Gritsaeva AV, Yanbaev FM, Simakin AV, Gudkov SV. Review of Antimicrobial Properties of Titanium Dioxide Nanoparticles. Int J Mol Sci. 2024;25(19):10519.
24. Brand-Williams W, Cuvelier ME, Berset C. Use of a free radical method to evaluate antioxidant activity. LWT - Food Science and Technology. 1995;28(1):25-30.
25. Aldwimi IM, Alhareb AO, Akil HM. Effect of HNTs and MWCNTs nanotubes on the impact strength and hardness of PMMA denture base. AIP Conference Proceedings: AIP Publishing; 2021. p. 100001.
26. Vuluga Z, Corobea MC, Elizetxea C, Ordonez M, Ghiurea M, Raditoiu V, et al. Morphological and Tribological Properties of PMMA/Halloysite Nanocomposites. Polymers. 2018;10(8):816.
27. Alamgir M, Mallick A, Nayak GC, Tiwari SK. Development of PMMA/TiO_2 nanocomposites as excellent dental materials. Journal of Mechanical Science and Technology. 2019;33(10):4755-4760.
28. Chand N, Siddiqui N. Improvement in thermo mechanical and optical properties of in situ synthesized PMMA/TiO_2 nanocomposite. Compos Interfaces. 2012;19(1):51-58.
29. Mahmood RS, Salman SA, Bakr NA. Optical, Thermal Properties of Cadmium Chloride Reinforced PVA:PVP Blend Films. Journal of Polymer and Composites. 2020:46-52.
30. Al-Muntaser AA, Alzahrani E, Abo-Dief HM, Saeed A, Alshammari EM, Al-Harthi AM, et al. Tuning the structural, optical, electrical, and dielectric properties of PVA/PVP/CMC ternary polymer blend using ZnO nanoparticles for nanodielectric and optoelectronic devices. Opt Mater. 2023;140:113901.
31. Salman SA, Bakr NA, Abduallah SS. Study of Thermal Decomposition and FTIR for PVA-AlCl3 Composite Films. Journal of Engineering and Applied Sciences. 2019;14(3):717-724.
32. Teng H, Koike K, Zhou D, Satoh Z, Koike Y, Okamoto Y. High glass transition temperatures of poly(methyl methacrylate) prepared by free radical initiators. J Polym Sci, Part A: Polym Chem. 2008;47(1):315-317.
33. Safi IN. Evaluation the Effect of Nano - Fillers (TiO_2, AL_2O_3, SiO_2) Addition on Glass Transition Temperature , E - Moudulus and Coefficient of Thermal Expansion of Acrylic Denture Base Material. Journal of Baghdad College of Dentistry. 2014;26(1):37-41.
34. Abaci U, Guney HY, Yilmazoglu M. Plasticizer effect on dielectric properties of poly(methyl methacrylate)/titanium dioxide composites. Polym Polym Compos. 2021;29(9_suppl):S565-S574.
35. Baliyan S, Mukherjee R, Priyadarshini A, Vibhuti A, Gupta A, Pandey RP, et al. Determination of Antioxidants by DPPH Radical Scavenging Activity and Quantitative Phytochemical Analysis of Ficus religiosa. Molecules. 2022;27(4):1326.
36. Gulcin İ, Alwasel SH. DPPH Radical Scavenging Assay. Processes. 2023;11(8):2248.
37. Blessymol B, Yasotha P, Kalaiselvi V, Gopi S. An antioxidant study of Titanium dioxide (TiO_2) nanoparticles against mace of nutmeg in Myristica fragrans houtt, rhizomes of Curcuma longa linn and Kaempferia galanga extracts. Results in Chemistry. 2024;7:101291.
38. Tiwari AK, Singh AK, Jha S, Tripathi SK, Awasthi RR, Mishra SK, et al. Green synthesis of TiO_2 nanoparticles using Kinnow peel extracts and their antioxidant properties. Sci Rep. 2025;15(1).
39. Chraibi M, Farah A, Balouiri M, Barkai H, Sadiki M, Benbrahim K. Chemical characterization and antimicrobial activity of Moroccan Pelargonium asperum essential oil. Journal of Applied Pharmaceutical Science. 2016:042-046.
40. Simakin AV, Burmistrov DE, Baimler IV, Gritsaeva AV, Serov DA, Astashev ME, et al. TiO_2 Nanoparticles Obtained by Laser Sintering When Added to Methacrylate Photopolymer Resin Improve Its Physicochemical Characteristics and Impart Antibacterial Properties. Inorganics. 2025;13(7):233.
41. Rosli NA, Teow YH, Mahmoudi E. Current approaches for the exploration of antimicrobial activities of nanoparticles. Science and Technology of Advanced Materials. 2021;22(1):885-907.
42. Ahmad N, Jafri Z, Khan ZH. Evaluation of nanomaterials to prevent oral Candidiasis in PMMA based denture wearing patients. A systematic analysis. Journal of Oral Biology and Craniofacial Research. 2020;10(2):189-193.
43. Gómez-Hernández ME, Baltierra-Uribe SL, Castillo-Cruz J, Mondragón-Flores R, González-Pozos S, Vidales-Hurtado MA, et al. Antifungal effect of titanium oxide nanoparticles on Candida glabrata internalized in human macrophages. Frontiers in Cellular and Infection Microbiology. 2025;15.
44. Priyanka KP, Sukirtha TH, Balakrishna KM, Varghese T. Microbicidal activity of TiO_2 nanoparticles synthesised by sol–gel method. IET Nanobiotechnology. 2016;10(2):81-86.
45. Abdul Jalill RD. Green synthesis of titanium dioxide nanoparticles with volatile oil of Eugenia caryophyllata for enhanced antimicrobial activities. IET Nanobiotechnology. 2018;12(5):678-687.
46. Li J, Zhang D, Hou C. Application of Nano-Titanium Dioxide in Food Antibacterial Packaging Materials. Bioengineering. 2024;12(1):19.